The Astrophysical Journal, 587:727–738, 2003 April 20

THE EFFECTS OF ION IRRADIATION ON THE EVOLUTION OF THE CARRIER OF THE 3.4 MICRON INTERSTELLAR ABSORPTION BAND

V. Mennella,[1] G. A. Baratta,[2] A. Esposito,[3] G. Ferini,[2] and Y. J. Pendleton[4]

Received 2002 July 26; accepted 2002 December 27

ABSTRACT

Carbon grains in the interstellar medium evolve through exposure to UV photons, heat, gas, and cosmic rays. Understanding their formation, evolution, and destruction is an essential component of evaluating the composition of the dust available for newly forming planetary systems. The 3.4 μm absorption band, attributed to the aliphatic C—H stretch vibration, is a useful probe of the degree to which energetic processing affects hydrogenated carbon grains. Here we report on the effects of ion bombardment of two different kinds of nano-size hydrogenated carbon grains with different hydrogen content. Grain samples, both with and without a mantle of H_2O ice, were irradiated with 30 keV He^+ to simulate cosmic-ray processing in both diffuse and dense interstellar medium conditions. The ion fluences ranged between 1.5×10^{13} and 7.9×10^{15} ions cm^{-2}. Infrared and Raman spectroscopy were used to study the effects of ion irradiation on grains. In both the dense and diffuse interstellar medium simulations, ion bombardment led to a reduction of the 3.4 μm band intensity. To discuss the effects of cosmic-ray irradiation of interstellar hydrogenated carbon materials we adopt the approximation of 1 MeV monoenergetic protons. An estimate of the C—H bond destruction cross section by 1 MeV protons was made based on experiments using 30 keV He^+ ions and model calculations. In combination with results from our previous studies, which focused on UV irradiation and thermal H atom bombardment, the present results indicate that the C—H bond destruction by fast-colliding charged particles is negligible with respect to that of UV photons in the diffuse ISM. However, in dense cloud regions, cosmic-ray bombardment is the most significant C—H bond destruction mechanism when the optical depth corresponds to values of the visual extinction larger than $\sim$5 mag. The results presented here strengthen the new interpretation of the evolution of the interstellar aliphatic component (i.e., the C—H bonds in the CH_2 and CH_3 groups) as evidenced by the presence of the 3.4 μm absorption band in the diffuse medium and the absence of such a signature in the dense cloud environment. The evolutionary transformation of carbon grains, induced by H atoms, UV photons, and cosmic rays, indicates that C—H bonds are readily formed, in situ, in the diffuse interstellar medium and are destroyed in the dense cloud environment.

Subject headings: astrochemistry — cosmic rays — dust, extinction — infrared: ISM — ISM: lines and bands — methods: laboratory

1. INTRODUCTION

Infrared spectroscopy has proven to be a powerful probe of the chemical composition of interstellar dust, with significant progress being made through combined efforts in the laboratory and at the telescope. The physical and chemical changes occurring within dust grains in the dense and diffuse interstellar medium are revealed through absorption and emission bands, and the evolution of carbonaceous material in the interstellar medium is becoming clearer.

One of the primary spectral signatures of the organic component of interstellar dust is the aliphatic carbon component observed in the diffuse interstellar medium (DISM) in absorption at 3.4 μm (2940 cm^{-1}; Adamson, Whittet, & Duley 1990; Sandford et al. 1991; Pendleton et al. 1994; Whittet et al. 1997; Pendleton & Allamandola 2002). The evolution of dust can be investigated through studies of this band (and its related counterparts), and in this paper we present new laboratory results that illustrate the effect of cosmic rays on hydrogenated carbonaceous materials in dense and diffuse clouds.

Since its detection along the line of sight toward infrared source number 7 in the Galactic center by Willner et al. (1979) and Wickramasinghe & Allen (1980), follow-up studies have shown that this material is likely a common DISM component in the Milky Way and other galaxies (Wright et al. 1996; Pendleton 1996a, 1996b; Imanishi 2000; Imanishi & Dudley 2000). The band profile is characterized by three subfeatures at about 3.38, 3.42, and 3.48 μm (2955, 2925, and 2870 cm^{-1}), typical of the C—H stretching modes in the methyl (CH_3) and methylene (CH_2) aliphatic groups.

The IR activity of the C—H stretching modes is accompanied by the activity of the bending modes around 7 μm. The *Infrared Space Observatory* spectra of dust along the line of sight toward the Galactic center source Sgr A* have recently provided conclusive evidence for the C—H bending modes at 6.85 and 7.25 μm associated with the 3.4 μm band (Chiar et al. 2000). These observations confirm the detection of the 6.85 μm band in the spectrum of the Galactic center and the upper limits placed on the diffuse ISM features toward the bright source Cyg OB2 12 from earlier data obtained with the Kuiper Airborne Observatory (Pendleton 1995; Tielens et al. 1996; Pendleton & Allamandola 2002). The presence of an additional broad absorption band,

[1] Istituto Nazionale di Astrofisica–Osservatorio Astronomico di Capodimonte, Via Moiariello, 16, 80131 Napoli, Italy.
[2] Istituto Nazionale di Astrofisica–Osservatorio Astrofisico di Catania, Via S. Sofia, 78, 95123 Catania, Italy.
[3] Università degli Studi di Napoli Parthenope, Via A. De Gasperi 5, 80133 Napoli, Italy.
[4] NASA Ames Research Center, Mail Stop 245-3, Moffett Field, CA 94035.

perhaps due to aromatic hydrocarbons, at ~3.3 μm in the spectra of IR sources near Sgr A* has recently been reported (Chiar et al. 2002).

The absorption band observed in the DISM at 3.4 μm has long been considered the result of energetic processing of icy grain mantles within dense molecular clouds (Greenberg 1978; Moore & Donn 1982; Greenberg et al. 1995). Given the short cycling time of dust between the diffuse and dense clouds (McKee 1989; Jones et al. 1994; Greenberg et al. 1995) and the widespread distribution of the carrier of the aliphatic signature throughout the diffuse ISM, the 3.4 μm band is expected to be present in the spectra of dense cloud dust; however, evidence of aliphatic hydrocarbons in the dense cloud dust has not been forthcoming (Brooke, Sellgren, & Smith 1996; Brooke, Sellgren, & Geballe 1999; Chiar, Adamson, & Whittet 1996). The absence of the 3.4 μm band was first noted by Allamandola et al. (1992, 1993), who pointed out that this discrepancy challenges our assumptions of processing that occurs in the two environments and places severe constraints on models of the formation and evolution of the interstellar aliphatic component. Muñoz Caro et al. (2001, hereafter Mu01) have estimated upper limits for the amount of the aliphatic hydrocarbon component that could be present in the dense cloud spectra. The upper limits indicate a reduction in the number of C—H bonds of at least 55% over those seen in the diffuse cloud environment. In the C—H stretching region of the dense cloud spectra, absorption signatures include the band at 3.47 μm, which has been attributed to tertiary C—H in dense clouds toward bright protostars (Allamandola et al. 1992) and in the quiescent cloud material (Chiar et al. 1996). Dense clouds do exhibit a strong 6.85 μm absorption signature, although the carrier of this band remains unknown. Analysis of the band profile toward different lines of sight suggests that both a volatile and a more refractory component contribute (Keane et al. 2001).

The 3.4 μm absorption band has not been detected in the spectrum of carbon-rich asymptotic giant branch stars, despite evidence for the presence of carbon particles in their atmospheres (Bagnulo, Doyle, & Griffin 1995), yet it has been observed in the more evolved C-rich protoplanetary nebula CRL 618 (Lequeux & Jourdain de Muizon 1990; Chiar et al. 1998). The striking similarity of the circumstellar feature to that observed in the diffuse medium toward the Galactic center suggests that at least some of the organic carriers that lead to the 3.4 μm absorption in the diffuse ISM originate as stardust (Chiar et al. 1998).

Spectropolarimetric observations have also shown that, unlike the 9.7 μm silicate band toward IRS 3, the 3.4 μm band along the line of sight toward Sgr A* (IRS 7) is not polarized (Adamson et al. 1999). The dust along this sight line is composed of both diffuse and dense material (Chiar et al. 2000), and both of these features have been attributed to the diffuse component. The difference in polarization suggests that there is no physical link between silicate grains and the carrier of the aliphatic feature in the diffuse interstellar medium and that the aliphatic band is probably produced by a separate population of very small (unaligned) grains (Adamson et al. 1999). However, observations of the 3.4 and 9.7 μm polarization for the same line of sight are necessary to draw a more solid conclusion on this aspect.

Much work has been carried out in the laboratory to identify the exact nature of the aliphatic material responsible for the interstellar feature in the diffuse ISM. Pendleton & Allamandola (2002) have recently performed a thorough comparative analysis of the spectrum of 13 analog materials in the range 2.5–10 μm with that of diffuse interstellar dust. They concluded that the organic refractory material in the diffuse ISM contains little oxygen and nitrogen and is much more similar to plasma-processed pure hydrocarbon materials than energetically processed ice residues. They find that the most carbon rich laboratory analogs, which possess clear aliphatic character but which also have a comparably strong aromatic component, provide the best agreement with the constraints derived from the current interstellar spectra.

Understanding the enigmatic difference of the 3.4 μm band between diffuse and dense medium has motivated additional laboratory simulations of carbon grain processing in space. The basic steps toward a new model for the evolution of the interstellar aliphatic component were (1) the finding that a 3.4 μm band is activated in carbon grains by exposure to hydrogen atoms (Mennella et al. 1999, hereafter Me99), (2) the high efficiency of energetic UV irradiation in destroying the C—H bonds both in simple hydrocarbon molecules (Mu01) and in hydrogenated carbon grains (Mennella et al. 2001, hereafter Me01), and (3) the estimation of the C—H bond formation cross section by H atoms in carbon grains (Mennella et al. 2002, hereafter Me02).

According to this interpretation, the presence of the aliphatic C—H bonds in diffuse clouds results from an equilibrium between destruction by UV photons and formation by H atoms (Mu01; Me01). Modeling of the evolution of the interstellar aliphatic component, based on the results of laboratory experiments, has shown that the equilibrium value for the hydrogenation of carbon grains under UV and H atom processing is obtained in a time interval 10^3 times smaller than the diffuse cloud lifetime $(3 \times 10^7$ yr), independently of the initial grain hydrogenation (Me02). This implies that the carrier of the 3.4 μm band (i.e., the C—H bonds in the CH_2 and CH_3 groups) that we observe today has formed in the diffuse interstellar medium itself and that there may be no direct connection between the C—H bonds observed in circumstellar environments and those responsible for the absorption in the diffuse medium. When grains cycle into a dense molecular cloud, they are further subjected to destructive processes (Galactic UV field at the cloud edges, cosmic rays, and internal UV fields farther in). However, in dense clouds, the presence of an ice mantle on the grains and the reduced amount of atomic hydrogen prevents the reformation of C—H bonds while their destruction by UV photons and cosmic rays can still proceed. These conclusions are indicated by the present work in the case of cosmic rays and from earlier work in the case of UV photons (Mu01; Me01).

Ion irradiation can deeply modify the properties of carbonaceous materials; see Compagnini & Calcagno (1994) for a thorough discussion of this subject. Ion beam analysis and residual gas analysis have shown that substantial hydrogen loss takes place as a result of ion bombardment of hydrogenated carbon films (Kalish & Adel 1989, and references therein). Spectroscopic studies have shown relevant changes after ion irradiation of the UV-visual spectrum of nanosized carbon grains with different structural properties (Mennella et al. 1997). Moreover, a reduction of the 3.4 μm band has been reported during ion irradiation of *a*-C:H films (e.g., Fujimoto et al. 1988; Gonzalez-Hernandez et al.

1988). Recently, Reynaud et al. (2001) have found that the aromatic and aliphatic C—H features of carbon nanopowder produced by IR laser pyrolysis of butadiene (C_4H_6) decrease with heavy ion irradiation.

The present paper reports the results of a systematic study of the transformations induced by 30 keV He^+ ions in hydrogenated carbon grains. To quantify the effects of ion irradiation we have estimated the cross section of C—H bond destruction by 30 keV He^+ ions from the decrease of the 3.4 μm band intensity as a function of the ion fluence. Based on the laboratory results, we discuss the influence of ion processing on the destruction of the aliphatic component in the ISM. In § 2 we describe the production, ion bombardment, and characterization by IR and Raman spectroscopy of the samples and present our results. These are discussed in § 3, while the implications for the evolution of the interstellar 3.4 μm band carrier are reported in § 4.

2. EXPERIMENT AND RESULTS

Two different kinds of hydrogenated carbon grains have been considered in the present work to ensure that the results are not specific to any one type of material. The first (hereafter ACH2) was prepared by condensation of carbon vapor obtained by striking an arc discharge between two carbon rods (Ultra Carbon, Ultra F Purity) in a 10 mbar hydrogen atmosphere. The carbon particles were collected on KBr substrates located 5 cm from the source. The resulting samples are characterized predominantly by chainlike aggregates composed of spherical grains with an average diameter of 10 nm. Rare forms of poorly graphitized carbon, bucky structures, and graphitic structures are also observed (Rotundi et al. 1998). The second type of grains was prepared in two phases. First, hydrogen-free carbon grains (hereafter ACARL) were produced by laser ablation of carbon electrodes in a 10 mbar argon atmosphere. The carbon vapor condensate was collected on similar substrates and at the same distance from the target as ACH2. The morphology of these samples is also characterized by chainlike aggregates of spherical grains with an average diameter of 10 nm (Me99). Hydrogenation of ACARL was obtained by exposure to hydrogen atoms produced by microwave-excited dissociation of molecular hydrogen. The H atom fluence was 4.2×10^{18} H atoms cm^{-2} for the samples considered in the present work. In the following we refer to these hydrogenated grains as ACARL_H. The absorption coefficient per unit mass at 2925 cm^{-1} of ACARL_H is about 1.6×10^3 cm^2 g^{-1}, and the estimated upper limit for the H/C atom ratio is 0.65. ACH2 is characterized by a lower absorption coefficient at 2925 cm^{-1}, 1.5×10^2 cm^2 g^{-1}, from which an estimation of the H/C = 0.1 was obtained using the same absorption cross section as that of ACARL_H (Me02). For more details on the properties of these hydrogenated grains we refer the reader to previous work (Colangeli et al. 1995; Me02).

To study the effects induced in hydrogenated carbon grains by ion processing, samples of both materials were irradiated with 30 keV He^+ ions at a pressure of 10^{-7} mbar. Details of the experimental setup have been described earlier (Strazzulla, Baratta, & Palumbo 2001). The samples were mounted on a cold finger at an angle of 45° with both the ion beam and the IR beam of a Fourier transform IR spectrophotometer (Bruker model Equinox 55) to monitor the IR spectral evolution of the samples during irradiation. In addition to unpolarized spectra, a polarizer placed in the optical path of the incoming IR beam allows the transmission measurements with the electric vector parallel (*p*-polarized) and perpendicular (*s*-polarized) to the plane of incidence. A resolution of 1 cm^{-1} was used. The ion beam was produced by an ion implanter (Danfysik model 1080-30). It was electrically swept in order to perform a homogeneous irradiation of the sample. During the experiments the average ion flux was 3.5×10^{11} ions cm^{-2} s^{-1} with the exception of experiment 7 (see Table 1), when a value of 9.5×10^{11} ions cm^{-2} s^{-1} was reached. The samples have been irradiated with fluences in the range 1.5×10^{13} to 7.9×10^{15} ions cm^{-2}. The maximum ion fluence, F_{max}, is reported in column (5) of Table 1.

The irradiation experiments were aimed at simulating cosmic-ray processing of grains under dense and diffuse medium conditions. In the first case, to reproduce the icy mantle present on grains in dense regions, a water ice layer was deposited on carbon grain samples at 12 K. The thickness, d_{H_2O}, of the ice layer was derived from the 3 μm band intensity, using a band absorbance of 2×10^{-16} cm mol^{-1} (Allamandola, Sandford, & Valero 1988) and a density of 1 g cm^{-3}. It is listed in column (4) of Table 1. Bare carbon samples were irradiated to mimic the diffuse interstellar medium conditions.

The evolution of the sp^3 C—H stretching band at 3.4 μm is shown in Figure 1 for two of the diffuse medium analog samples (ACH2-1 and ACARL_H-4), at three stages: before irradiation, at an intermediate ion fluence, and after the maximum ion processing. As a result of ion irradiation the intensity of the feature is strongly reduced. A similar spectral evolution was observed for the two dense medium

TABLE 1

30 keV He^+ Ion Irradiation of Hydrogenated Carbon Grains

Number	Sample	Temperature (K)	d_{H_2O} (nm)	F_{max} (10^{15} ions cm^{-2})	$\tau_{3.4\,\mu m,i}$ (cm^{-1})	$\tau_{3.4\,\mu m,f}$ (cm^{-1})	$\tau_{3.4\,\mu m,r}$ (cm^{-1})	σ_d (10^{-15} cm^2 ion^{-1})
1.....	ACARL_H-1	300	...	3.4	1.54	0.55	0.96 ± 0.02	2.4 ± 0.2
2.....	ACARL_H-2	12	35	2.7	2.14	0.46	1.67 ± 0.03	2.8 ± 0.3
3.....	ACARL_H-3	300	...	3.4	1.07	0.21	0.83 ± 0.02	5.1 ± 0.6
3 bis	ACARL_H-3	12	57	1.7	0.21	0.14	0.074 ± 0.003	5.2 ± 1.3
4.....	ACARL_H-4	300	...	3.6	1.75	0.26	1.47 ± 0.02	3.9 ± 0.4
4 bis	ACARL_H-4	12	8	1.9	0.24	0.10	0.137 ± 0.005	5.7 ± 1.4
5.....	ACH2-1	300	...	7.9	0.78	0.24	0.51 ± 0.02	1.24 ± 0.14
6.....	ACH2-2	300	...	4.2	0.65	0.22	0.44 ± 0.01	1.19 ± 0.05
7.....	ACH2-3	12	46	4.8	0.64	0.10	0.55 ± 0.01	0.94 ± 0.04

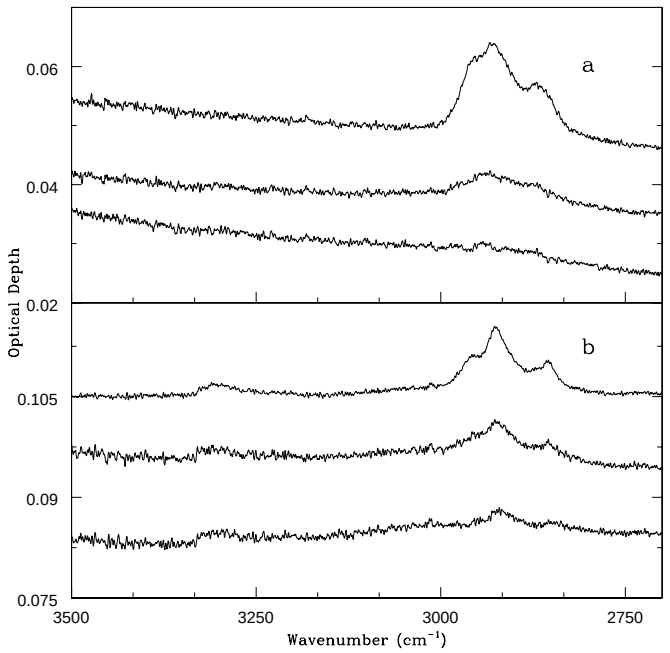

FIG. 1.—3.4 μm band of (*a*) ACARL_H-4 and (*b*) ACH2-1 before and after ion irradiation at fluences of 6.3×10^{14} and 3.6×10^{15} ions cm^{-2} (ACARL_H-4) and 3.9×10^{14} and 4.2×10^{15} ions cm^{-2} (ACH2). In both panels the spectra are offset from each other in ordinate for the sake of clarity. They are arranged by increasing fluence from top to bottom.

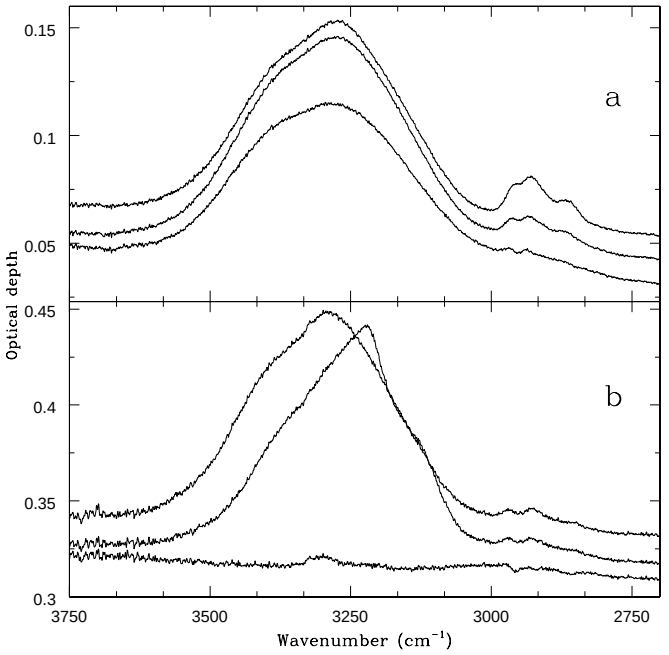

FIG. 2.—3 μm water ice band and 3.4 μm of (*a*) ACARL_H-2 and (*b*) ACH2-3 before and after ion irradiation at fluences of 5.1×10^{14} and 2.7×10^{15} ions cm^{-2} (ACARL_H-2) and 1.4×10^{14} and 4.8×10^{15} ions cm^{-2} (ACH2-3). In both panels the spectra are offset from each other in ordinate for the sake of clarity. They are arranged by increasing fluence from top to bottom. In the case of ACH2-3 the evolution of the 3 μm feature indicates crystallization and sublimation of the ice cap. This temperature effect can be interpreted in terms of sample heating caused by the higher ion current used in this experiment (see text).

analog samples, ACH2-3 and ACARL_H-2 (see Fig. 2). The intensity reduction of the C—H stretching band is accompanied by that of the corresponding bending modes at 1457 and 1378 cm^{-1}. Unlike the sp^3 C—H stretching band, the intensity of the weak sp^1 C—H stretching feature at 3306 cm^{-1}, present in the spectrum of ACH2, does not vary with ion fluence (see Figs. 1 and 2). Ion irradiation also reduces the intensity of the carbonyl C═O stretch at 1720 cm^{-1}. The presence of this band and its variation during irradiation make it difficult to evaluate the changes, if any, of the weak C—C band at $\sim$1600 cm^{-1}. In addition, when a water layer is present on the samples, the O—H bending band at 1600 cm^{-1} masks the other features falling in this spectral range. Moreover, a band at 2106 cm^{-1}, due to the C≡C stretch of alkynes, develops and stabilizes with ion processing in the spectrum of both kinds of grains, independent of a water ice layer. Finally, the bands at 2341 and 2140 cm^{-1}, due to CO_2 and CO, respectively, develop during irradiation of the samples when a water ice cap is present. The formation of CO_2 and CO is at present being investigated in detail (V. Mennella et al. 2003, in preparation).

As seen in Figure 2, the O—H stretching band at 3300 cm^{-1} exhibits a different behavior in the ACH2-3 and ACARL_H-2 samples. As a result of ion sputtering and condensation of the water vapor of the background gas, it does not change significantly during irradiation of the ACARL_H-2 sample. On the other hand, the band systematically decreases in the case of ACH2-3. As one can see in Figure 2, the feature becomes sharper and asymmetric and its peak position shifts from 3300 to 3224 cm^{-1} after an irradiation of 1.9×10^{14} ions cm^{-2}. At the maximum ion fluence considered, 4.8×10^{15} ions cm^{-2}, there is no spectroscopic evidence for any water ice layer on the carbonaceous deposit. These variations are similar to those found during annealing of amorphous water ice deposited at 12 K, when crystallization (at 140–160 K) and, then, sublimation of the ice (at 160–170 K) take place with increasing temperature (e.g., Baratta et al. 1991; Strazzulla et al. 1992). Therefore, we interpret the evolution of the O—H stretching band at the 3 μm band in terms of sample heating caused by the higher ion current used in this experiment (see above). It is worth noting that such effects have never been observed for water ice deposited on silicon substrates, even at much higher ion current. This implies that the fluffy morphology of carbon grains does not allow a good thermal contact with the cold substrate, resulting in the observed sample heating.

The detailed evolution with ion fluence of the integrated intensity of the 3.4 μm band, $\tau_{3.4\,\mu m}$, is shown in Figures 3 and 4, respectively, for ACARL_H and ACH2. In these figures, the points represent the averages, with their errors, of several integrations of the band profile obtained with different choices of the baseline. In general, after a fast reduction at low ion fluences, $\tau_{3.4\,\mu m}$ decreases less and less and stabilizes at a constant value as the ion fluence increases. The initial band intensity, $\tau_{3.4\,\mu m,i}$, and that obtained after the maximum fluence considered in each experiment, $\tau_{3.4\,\mu m,f}$, are reported, respectively, in columns (6) and (7) of Table 1. The reduction of the band intensity after ion bombardment ranges from 65% to 85% for both kinds of hydrogenated carbon grains. After irradiation at room temperature of the ACARL_H-3 and ACARL_H-4 samples, we lowered the temperature to 12 K and deposited a water ice layer of 57 and 8 nm, respectively. Further irradiation at ion fluences of 1.7×10^{15} and 1.9×10^{15} ions cm^{-2} resulted in an

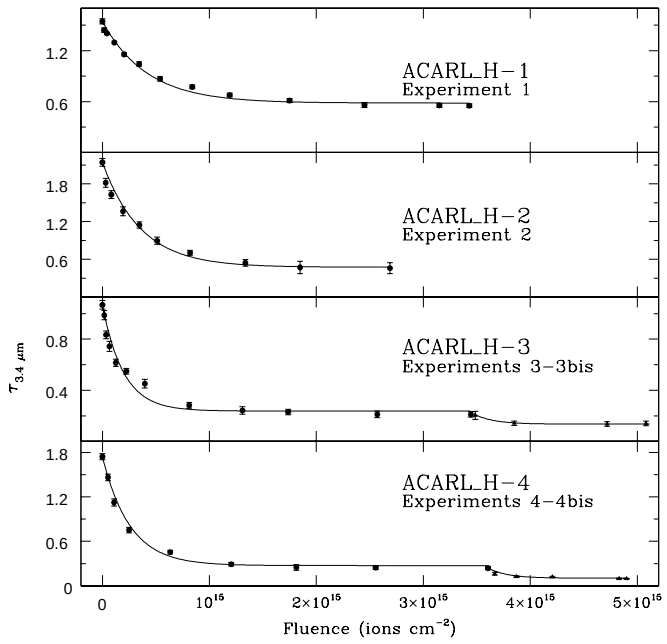

FIG. 3.—Evolution of the 3.4 μm band intensity with ion irradiation of ACARL_H for different experiments.

exponential decrease of $\tau_{3.4\,\mu m}$ with ion fluence from the asymptotic value to a new equilibrium value: from 0.21 to 0.14 cm^{-1} and 0.26 to 0.10 cm^{-1} for ACARL_H-3 and ACARL_H-4, respectively (see Fig. 3 and Table 1 experiments 3 bis and 4 bis). At the end of irradiation of ACARL_H –4 we monitored the spectral evolution during warm-up of the sample. At 30 K the intensity of the 3.4 μm band increased from 0.10 to 0.18 cm^{-1}. A gradual increase continued very slowly up to 0.22 cm^{-1} for $T = 230$ K, until an exponential rise brought the band intensity to the constant value of 0.64 cm^{-1}.

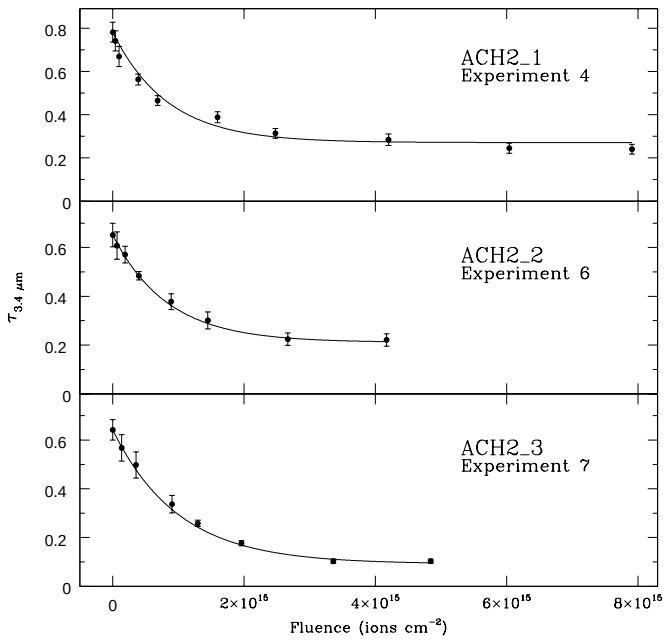

FIG. 4.—Evolution of the 3.4 μm band intensity with ion irradiation of ACH2 for different experiments.

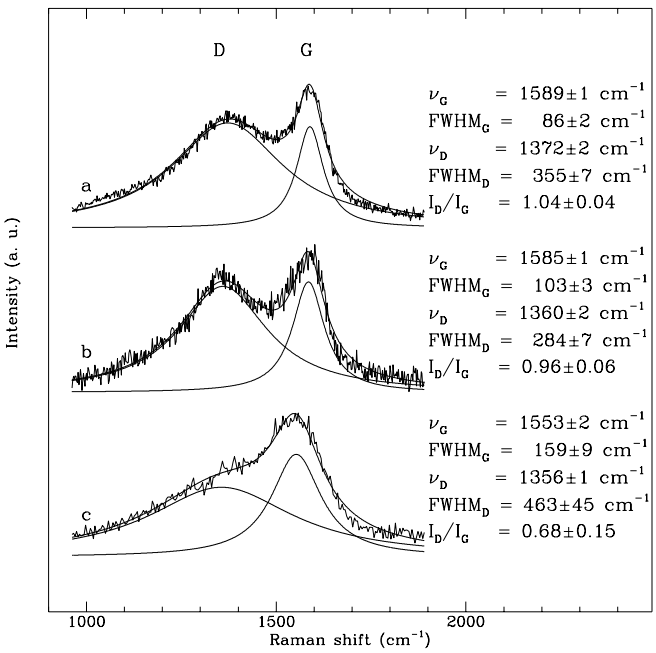

FIG. 5.—First-order G and D Raman bands of (a) hydrogen-free carbon grains ACARL and of ACARL_H carbon grains hydrogenated by exposure to atomic hydrogen (b) before and (c) after irradiation at a fluence of 1.3×10^{15} ions cm^{-2}. The fits to the spectra of the sum of two Lorentzian components and the single component are shown. The corresponding peak position (ν), the FWHM, and the intensity ratio of the D and G bands are also reported.

To understand the structural modifications induced by ion bombardment, we have performed Raman spectroscopy of the samples after ion irradiation. Raman spectra were measured at room temperature with a confocal optical system. The excitation source was the 514 nm line of an argon laser. The backscattered radiation was analyzed with a spectrometer (Triplemate SPEX 1877) equipped with a photomultiplier. Further details on the experimental setup are reported in Strazzulla et al. (2001). The evolution with ion irradiation of the first-order G and D Raman lines typical of carbonaceous materials is shown in Figures 5 and 6 for ACARL_H and ACH2, respectively. The fitting curves, the Lorentzian components, and the corresponding parameters resulting from a line shape fitting analysis of the spectra are also shown. In Figure 5, the spectrum of ACARL grains before exposure to atomic hydrogen is reported for comparison. The spectral comparison and the variations of the fitting parameters of ACARL and ACARL_H indicate no changes, within the errors, of the intensity ratio of the D and G lines, I_D/I_G, and small variations of peak positions and widths of the two bands. On the other hand, ion irradiation produces significant variations of the Raman spectrum of the hydrogenated carbon grains ACARL_H (see Fig. 5). In fact, I_D/I_G decreases, the G band becomes broader and shifts toward lower frequency, and the D line widens and becomes a shoulder of the G line. Unlike ACARL_H, the evolution with ion irradiation of ACH2 is characterized by a constant value, within the errors, of I_D/I_G and by the narrowing of the G line that shifts toward lower wavenumbers (see Fig. 6). Moreover, the D line becomes broader and falls at higher Raman shifts after irradiation. We note that, unlike all the other samples studied in the present work,

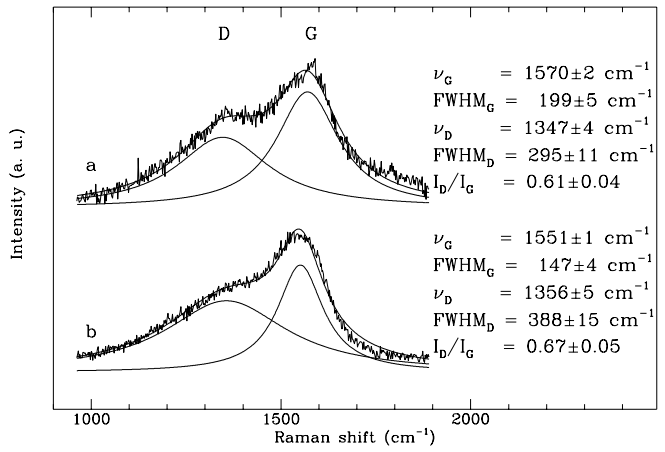

FIG. 6.—First-order *G* and *D* Raman bands of hydrogenated carbon grains ACH2 (*a*) before and (*b*) after irradiation at a fluence of 4.2×10^{15} ions cm^{-2}. The fits to the spectra of the sum of two Lorentzian components and the single component are shown. The corresponding peak position (ν), FWHM, and the intensity ratio of the *D* and *G* bands are also reported.

ACH2, which was not irradiated, was easily annealed by the laser radiation used to induce Raman emission. We tried to minimize this effect by reducing the laser power and dispersing the grains in a Raman-inactive KBr matrix. Actually, the aromatic clustering degree of ACH2 could be lower than its first-order Raman spectrum indicates because of the laser annealing. Finally, it is worth stressing that the spectrum of ACARL_H after irradiation of a fluence of 7.0×10^{15} ions cm^{-2} perfectly matches that of ACH2 irradiated with 4.2×10^{15} ions cm^{-2}.

3. DISCUSSION

When a fast ion collides with a solid target, it produces several effects such as sputtering, structural modifications, and changes of the chemical properties (e.g., Johnson 1998; Strazzulla 1998). These effects are induced by the ion energy loss due to elastic collisions with the target nuclei and inelastic collisions with electrons, which produce ionization and excitations. The energy deposited by the ion is characterized by the stopping power, dE/dx, which is defined as the energy deposited per unit path length as it moves through the solid. Related to the stopping power is the stopping cross section, $S = (dE/dx)\rho^{-1}$, where ρ is the target density. It consists of an electronic (inelastic) and nuclear (elastic) term. Nuclear stopping is dominant at low energies, while electronic energy loss prevails at high ion speeds. Moreover, the relative importance of the two kinds of energy deposition depends on the atomic mass of both colliding ions and target atoms (e.g., Johnson 1990).

In the case of hydrogenated carbon grains the stopping cross section depends on the H/C ratio. Using the Monte Carlo code TRIM, we have calculated a stopping cross section of 30 keV He^+ ions, $S_{30\,keV,He^+} = 830$ MeV cm^2 g^{-1}, for H/C = 0.67. The contribution of the nuclear part to $S_{30\,keV,He^+}$ is less than 5%. The stopping cross section varies during irradiation since the H/C ratio decreases with ion fluence. However, a reduction of H/C from 0.67 to 0 yields only a 10% decrease of $S_{30\,keV,He^+}$; thus, we neglect this variation and adopt the value $S_{30\,keV,He^+} = 830$ MeV cm^2 g^{-1} as a constant during irradiation for both ACARL_H and ACH2. By definition, the dose deposited in a sample is the product of the stopping power times the ion fluence, so the maximum fluence of each experiment listed in Table 1, when multiplied by the factor 830 MeV cm^2 g^{-1}, corresponds to the maximum dose deposited in the sample. In addition, using the code TRIM, we have estimated a mean path length (the range) of 30 keV He^+ ions of ~300 nm in our hydrogenated carbon grains. Also in this case the small dependence of the range on the H/C ratio has been neglected.

The changes induced in the spectra of our samples by ion irradiation are clear evidence for the destruction of C—H bonds. We interpret the reduction of the band intensity as a direct reduction of the C—H bonds during ion irradiation because the samples considered in the present work are optically thin at 3.4 μm. Structural variations are expected during ion irradiation. However, the changes of the C—H stretching probe only the local bonding configuration of carbon atoms. Raman scattering is very sensitive to the structural disorder that breaks the translational symmetry of bulk crystals that occurs in disordered carbonaceous materials. As a result of the work by Tuinstra & Koenig (1970), the intensity ratio of the first-order *D* and *G* lines, I_D/I_G, can be considered as a parameter for probing the structural properties of carbonaceous materials. These authors found that for polycrystalline graphites, I_D/I_G is proportional to the inverse of the aromatic coherence length of the graphitic clusters, L_a. However, successive studies have shown that this relation is no longer valid for disordered carbon materials containing very small sp^2 clusters. Thermal annealing experiments on very disordered hydrogenated carbon films have indeed showed that the intensity ratio of the two first-order Raman bands initially increases, then reaches a maximum, and finally decreases with increasing annealing temperature (Dillon, Woollam, & Katkanant 1984). A similar evolution of I_D/I_G has been observed during thermal annealing of ACH2 (Mennella et al. 1995). This trend with temperature is equivalent to that with L_a, since thermal annealing is a process that induces a monotone increase of the average size of sp^2 clusters. The value of L_a corresponding to the maximum of I_D/I_G is between 12 and 16 Å (Tamor et al. 1989; Robertson 1991). In addition to the variations of I_D/I_G the width and the position of the two bands vary with disorder. They widen, and the *G* line shifts from ~1590 cm^{-1} toward lower frequencies (~1560 cm^{-1}) as disorder increases. In the Raman spectrum of disordered carbons the two features are not resolved and the *D* line appears as a shoulder of the *G* line.

On the basis of these considerations we can infer information on the structural changes of our samples from the variations of the Raman spectra of Figures 5 and 6. First, we note that Raman spectroscopy indicates that the hydrogen-free grains ACARL are quite ordered from the structural point of view. Their marked graphitic character is also revealed by the properties of the IR spectrum (Me99). Exposure of ACARL to atomic hydrogen does not significantly affect the structural properties, although it induces a considerable degree of hydrogenation (H/C ~ 2/3) and the activation of the aliphatic C—H stretching and bending IR bands. Me02 concluded that the aliphatic carbon component is a minor part in ACARL processed by H atoms even for high H/C ratios. The present Raman spectra show that the other carbon atoms in these hydrogenated carbon grains

remain mainly organized in aromatic sp^2 clusters. Ion processing produces a decrease of the sp^2 clustering degree of the hydrogenated carbon grains ACARL_H as shown by the changes of the Raman activity after ion irradiation. This amorphization is caused by the so-called displacement collisions, and its efficiency depends on the sp^2 cluster size: it becomes more and more important as the structural order increases (Compagnini, Calcagno, & Foti 1992; Baratta et al. 1996).

The comparison of the Raman spectra points out that ACARL_H is more ordered than ACH2, despite the possible bias caused by laser annealing during acquisition of the Raman spectrum of ACH2 (see previous section). The low sp^2 clustering degree suggested by the first-order Raman spectrum of ACH2 agrees with the UV-visual and IR spectral properties of these grains and with their evolution under thermal annealing (Colangeli et al. 1995; Mennella et al. 1995). The variations of the Raman activity after irradiation indicate an increase of the sp^2 clustering degree, i.e., graphitization of grains, and are in agreement with the analysis of the evolution with ion irradiation of the UV-visual spectrum of ACH2 (Mennella et al. 1997). Graphitization is related to the energy release in the form of heat (thermal spikes) inside the collision cascade produced by impinging ions that transforms sp^3 into sp^2 sites with or without hydrogen loss (Compagnini & Calcagno 1994). Finally, we note that the striking similarity of the Raman spectrum of ACH2 and ACARL_H after ion irradiation reflects the equilibrium that sets in between graphitization and amorphization at high ion fluences: carbon materials with different starting structural properties tend to have similar properties after ion bombardment (Compagnini & Calcagno 1994).

3.1. *Estimation of the Destruction Cross Section of* C—H *Bonds by Ion Irradiation*

In order to quantify the effects of ion bombardment we have estimated the cross section of C—H bond destruction by 30 keV He^+ ions, $\sigma_{d,\mathrm{ions}}$, from the intensity decrease of the 3.4 μm band as a function of the ion fluence. Under the hypothesis of a first-order kinetic process we have

$$\frac{d\tau_{3.4\,\mu\mathrm{m}}}{dt} = -\sigma_{d,\mathrm{ion}}\Phi_{\mathrm{ion}}\tau_{3.4\,\mu\mathrm{m}} \ , \qquad (1)$$

where Φ_{ion} (ions cm^{-2} s^{-1}) is the flux of 30 keV He^+ ions on the sample, $\sigma_{d,\mathrm{ion}}$ (cm^2 ion^{-1}) is the destruction cross section of C—H bonds per ion, and t is the time. The solution of equation (1) is

$$\tau_{3.4\,\mu\mathrm{m}}(t) = \tau_{3.4\,\mu\mathrm{m},i}e^{-\sigma_{d,\mathrm{ion}}\Phi_{\mathrm{ion}}t} \ , \qquad (2)$$

where $\tau_{3.4\,\mu\mathrm{m},i}$ is the band intensity for $t = 0$.

Equation (2) predicts a complete C—H bond destruction for high fluences; however, it cannot reproduce the experimental trends of the $\tau_{3.4\,\mu\mathrm{m}}$ with ion fluence since $\tau_{3.4\,\mu\mathrm{m}}$ stabilizes to asymptotic values that are different from zero. A similar trend for the 3.4 μm band intensity was found during UV irradiation of hydrogenated carbon grains (Me01). In that case the residual intensity at high UV fluences was interpreted in terms of contribution of the unprocessed deepest layers of the samples, which were optically thick for UV photons. To take into account the nonuniform processing of UV irradiation in the samples equation (2) was modified as follows:

$$\tau_{3.4\,\mu\mathrm{m}} = \tau_{3.4\,\mu\mathrm{m},f} + \tau_{3.4\,\mu\mathrm{m},r}e^{-\sigma_{d,\mathrm{ion}}\Phi_{\mathrm{ion}}t} \ . \qquad (3)$$

The asymptotic value $\tau_{3.4\,\mu\mathrm{m},f}$ represents the residual 3.4 μm band intensity for long UV irradiation times, due to the unprocessed deeper layers of the samples; $\tau_{3.4\,\mu\mathrm{m},i} = \tau_{3.4\,\mu\mathrm{m},f} + \tau_{3.4\,\mu\mathrm{m},r}$ is the initial band intensity, and $\tau_{3.4\,\mu\mathrm{m},r}$ is the maximum reduction for the band intensity.

To see whether such an interpretation is applicable to the results of the present experiments we have to compare the sample thickness with the range of 30 keV He^+ ions in the materials we have studied. Although a precise determination of the thickness of the samples is not possible because of their morphology, a rough estimation of the effective thickness can be obtained from the optical depth of the samples at 3.4 μm. Using a density of 1.5 g cm^{-3} and the absorption coefficient per unit mass of the 3.4 μm band for ACARL_H and ACH2 (Colangeli et al. 1995; Me02) we obtain a thickness of 70 and 50 nm for ACARL_H-2 and ACH2_1, respectively. These samples have the highest optical depth among those we have considered (see Table 1). These quantities are smaller than the mean path length of the ions (300 nm; see § 3), and, consequently, ion processing should be considered uniform, even if we cannot exclude that a minor part of the sample may not receive radiation because of the sample morphology. This conclusion remains valid also for dense medium analog samples, since the ice thickness is lower than the range ($\sim$500 nm) of 30 keV He^+ ions in water ice.

The presence of a residual intensity of the aliphatic feature at high ion fluences may have a different origin. Several studies of hydrogen release from *a*-C:H films indicate that substantial hydrogen loss takes place at relatively low irradiation fluences (10^{15} ions cm^{-2}). Independent of irradiation conditions, a saturation level for H/C of about 0.05–0.10 is reached when hydrogen loss stops (Kalish & Adel 1989 and references therein). To interpret this behavior, Adel et al. (1989) proposed a statistical model based on the recombination within the material of atomic to molecular hydrogen. H_2 molecules hardly recombine compared to hydrogen atoms and can diffuse out of the sample without further interactions. Hydrogen loss can also take place through the effusion of hydrocarbon molecules. Thermal effusion measurements of *a*-C:H films indicate that H_2 and/or hydrocarbon molecules are desorbed, depending on the film properties (Wild & Koidl 1987). For the formation of an H_2 molecule to occur, two H atoms coming from the breaking of two C—H bonds must recombine within a characteristic volume. This volume is given by the inverse of the final hydrogen volume density at which the hydrogen content reaches its asymptotic value. In addition to this parameter, the H-loss process is governed by an effective molecular release cross section. This model can account for the hydrogen concentration of *a*-C:H films as a function of ion irradiation.

The evolution of the 3.4 μm band intensity with ion fluence refers specifically to bonded hydrogen atoms. C—H and C—C bonds are broken as a result of the energy deposited by ions in hydrogenated carbon materials. The consequent rearrangement of the carbon bonding configuration has been discussed above. Concerning the free H atoms, in addition to the H_2 formation, they can recombine with C atoms and reform C—H bonds, or they can remain weakly bonded in the structure. Therefore, the formation as well as

destruction of C—H bonds must be considered during ion irradiation. At high ion fluences, the equilibrium value of the number of C—H bonds, and consequently the optical depth of the 3.4 μm band, depends on the rate of these two competitive processes. The formulation of a detailed model for these processes is beyond the aim of the present work. However, we note that equation (3) represents the evolution under ion irradiation for the case in which the destruction of C—H bonds by ions is counteracted by the formation of a constant number of C—H bonds per unit mass and per unit time. The ratio of this quantity and the destruction rate of C—H bonds is proportional to the equilibrium value for $\tau_{3.4\,\mu\mathrm{m}}$ at high fluences. This consideration is of general validity and does not depend on the specific assumption.

As a first approximation, to reproduce the observed trends of $\tau_{3.4\,\mu\mathrm{m}}$ with ion irradiation we use equation (3). It can be expressed in terms of the initial band intensity $\tau_{3.4\,\mu\mathrm{m},i}$ and the band reduction, $\tau_{3.4\,\mu\mathrm{m},r}$, as

$$\tau_{3.4\,\mu\mathrm{m}} = \tau_{3.4\,\mu\mathrm{m},i} + \tau_{3.4\,\mu\mathrm{m},r}(e^{-\sigma_{d,\mathrm{ion}}\Phi_{\mathrm{ion}}t} - 1) \ . \qquad (4)$$

The best fits of equation (4) to the experimental data, using $\tau_{3.4\,\mu\mathrm{m},r}$ and $\sigma_{d,\mathrm{ion}}$ as adjustable parameters, are shown in Figures 3 and 4, while the best-fit parameters are reported in Table 1. For ACH2 the destruction cross sections obtained in the three experiments are very similar, and their weighted average is $(1.05 \pm 0.03) \times 10^{-15}$ cm^2 per ion. We consider this value as representative of $\sigma_{d,\mathrm{ion}}$ of bare ACH2 samples, since, as discussed above, ice sublimation took place during irradiation of ACH2-3. On the other hand, the values of $\sigma_{d,\mathrm{ion}}$ of ACARL_H are rather scattered for both the considered irradiation conditions. However, the weighted averages $\sigma_{d,\mathrm{ion}}$ are equal: $(2.9 \pm 0.2) \times 10^{-15}$ and $(3.0 \pm 0.3) \times 10^{-15}$ cm^2 ion^{-1}, respectively, for bare samples and for those with a water ice cap. The present results indicate that the destruction cross section of ACARL_H is a factor of 3 higher than that of ACH2. The difference can be interpreted as indication of a dependence of $\sigma_{d,\mathrm{ion}}$ on the hydrogen concentration of the material. This is in line with the results by Fujimoto et al. (1988) that found an increase of the decay rate of the hydrogen concentration with the initial hydrogen content of *a*-C:H films during elastic recoil detection of hydrogen with 12 MeV C^{+3} ions.

Finally, the exponential decrease of $\tau_{3.4\,\mu\mathrm{m}}$ from the asymptotic value reached during irradiation at room temperature to a lower equilibrium value after deposition of water ice and further irradiation (experiments 3 bis and 4 bis) can be interpreted as indication of a decrease of the number of C—H bonds that form during irradiation with respect to the corresponding irradiation at room temperature. A possible origin for the observed behavior is the lowering of the hydrogen diffusion that reduces the recombination of C—H bonds at low temperature with respect to room temperature. Moreover, the formation of CO and CO_2 could contribute to lower the recombination of C—H bonds by reducing the number of C atoms available to bind to hydrogen. The reformation of C—H bonds is testified by the evolution of the band intensity during warm-up of the ACARL_H-4. The abrupt increase of $\tau_{3.4\,\mu\mathrm{m}}$ at 30 K and its almost constant value between 30 and 230 K can be interpreted as recombination of free H atoms with carbon. Moreover, the increase of the band intensity for higher temperatures suggests a temperature-activated transformation of weakly bonded hydrogen atoms into C—H bonds.

4. THE EFFECTS OF ION IRRADIATION ON THE EVOLUTION OF THE INTERSTELLAR ALIPHATIC COMPONENT

To discuss the implications of the present irradiation experiments for the evolution of the interstellar 3.4 μm band, we assume that the hydrogenated carbon grains ACARL_H are representative of the carrier of the interstellar 3.4 μm band. This assumption is supported by (1) the good spectral match of the interstellar C—H stretching and bending features (Pendleton & Allamandola 2002; Me02); (2) the lowest amount of carbon among the analogs studied so far to reproduce the intensity of the aliphatic features; and (3) the production method that simulates hydrogenation of carbon particles by H atoms, likely the key mechanism to explain the presence of C—H bonds in the diffuse ISM. The 3.4 μm band profile of ACH2 can also match that of the interstellar aliphatic feature (see Fig. 3 of Me01); however, an unrealistic amount of carbon would be necessary to reproduce the interstellar band intensity, because of low absorption coefficient per unit mass of these hydrogenated carbon grains.

The basic parameter to discuss the effects of cosmic-ray processing on the evolution of the aliphatic component in the interstellar medium is the destruction rate of C—H bonds, which is defined as

$$R_{d,\mathrm{CR}} = \int_0^\infty \sum_k \sigma_{d,k}(E)\Phi'_k(E)dE \ , \qquad (5)$$

where $\sigma_{d,k}(E)$ is the C—H bond destruction cross section by the component K of cosmic rays with energy E, whose flux per unit energy is $\Phi'_k(E)$. The evaluation of $R_{d,\mathrm{CR}}$ requires the knowledge of the destruction cross sections for different ions and the corresponding interstellar fluxes. While the destruction cross section of a particular ion can be either estimated with specific experiments or derived from experiments performed with a different ion species (see below), the evaluation of the flux is much more problematic. The cosmic-ray flux is relatively well known at energies exceeding 100 MeV but is still quite uncertain at lower energy. No direct observations of low-energy Galactic cosmic rays are available, since the solar wind with its magnetic field tends to reflect the low-energy particles back into interstellar space. To discuss the effects of cosmic-ray irradiation of interstellar grains and ices, the approximation of monoenergetic protons has been adopted (e.g., de Jong & Kamijo 1973; Strazzulla & Johnson 1991; Jenniskens et al. 1993; Moore 1999; Moore, Hudson, & Gerakines 2001). This approximation relies on the estimation of a proton flux, usually at 1 MeV, from the cosmic-ray ionization rate, ζ_{CR}. Following this approach, we consider irradiation of 1 MeV protons to study cosmic-ray irradiation of interstellar hydrogenated carbon grains. We estimate the flux of these particles, $\Phi_p(1\ \mathrm{MeV}) \equiv \Phi_{p,1\,\mathrm{MeV}}$, as

$$\Phi_{1\,\mathrm{MeV}} = \frac{\zeta_{\mathrm{CR}}}{\sigma_{i,p}(1\ \mathrm{MeV})} \ , \qquad (6)$$

where $\sigma_{i,p}(1\ \mathrm{MeV})$ is the 1 MeV proton impact ionization cross section of atomic or molecular hydrogen, respectively, for diffuse or dense clouds. The $\Phi_{1\,\mathrm{MeV}}$ must be regarded as an effective quantity. It represents the flux of 1 MeV protons, which gives rise to the ionization rate produced by the

cosmic-ray spectrum if hydrogen were the only source for ionization. Protons of higher energy, for instance 100 MeV, could be adopted for this representation. In that case, the effective flux of protons would be higher than that at 1 MeV as the proton impact ionization cross sections of both atomic and molecular hydrogen decrease with energy. The influence of the choice of proton energy on the C—H bond destruction rate is discussed below. We note that in this approximation, a different cosmic-ray ion, for instance helium, could be used to describe the effects of cosmic-ray irradiation of hydrogenated carbon grains (see below for an example).

Low-energy ($\sim$1 MeV) protons, whose intensity and stopping power are higher in this energy range, are an important, but not the predominant, source of interstellar grain processing. Helium and high-mass ions, which are less abundant (Simpson 1983), can contribute significantly to the C—H bond destruction because their stopping power is higher than that of 1 MeV protons. In fact, the specific contribution of the different cosmic-ray ions to $R_{d,\mathrm{CR}}$, as a function E (the integrand function of eq. [5]), can be expressed as

$$dR_{d,\mathrm{CR}}(E) = \sigma_{d,p}(E)\Phi'_p(E)\left[\sum_k a_k b_k(E)\right]dE\ , \qquad (7)$$

where a_k is the abundance of the component K of cosmic rays relative to protons and $b_k(E)$ is its destruction cross section normalized to that of protons. In equation (7), the first term of the sum, with $a_1 = b_1 = 1$, refers to protons; $b_k(E)$ scales with energy like the normalized stopping power of the K component in hydrogenated carbon grains. Thus, using the abundances reported by Simpson (1983), the sum in equation (7) can be estimated with a sufficient degree of approximation. Here, for example, we report the contribution to C—H bond destruction of helium and carbon ions relative to protons: 1.13, 1.63, 1.0 and 0.03, 0.29, 0.16, respectively, at 1, 100, and 1000 MeV.

Like $R_{d,\mathrm{CR}}$, the cosmic-ray ionization rate is defined as a weighted integral over E of the cosmic-ray spectrum, with weighting functions being the ionization cross sections of interstellar gas species. Its evaluation is even more problematic than $R_{d,\mathrm{CR}}$. However, ζ_{CR} can be inferred from chemical modeling of the observed abundances of molecules such as HO, HD, and H_3^+. Estimations of ζ_{CR} ranging from $(2\text{–}3) \times 10^{-17}$ s^{-1} up to values a factor of 10 higher are reported for both diffuse and dense clouds (e.g., Kulkarni & Heiles 1987; Federman, Weber, & Lambert 1996; van der Tak & van Dishoeck 2000 and references therein). To estimate $\Phi_{1\,\mathrm{MeV}}$, we assume $\zeta_{\mathrm{CR}} = 6 \times 10^{-17}$ as a reference value for both these regions. Moreover, we use the proton impact ionization cross sections of atomic and molecular hydrogen, with the contribution of secondary ionization by electrons, reported by Spitzer & Tomasko (1968) and Cravens & Dalgarno (1978), respectively. The resulting values of $\Phi_{p,1\,\mathrm{MeV}}$ are 1 and 1.8 protons cm^2 s^{-1} for dense and diffuse regions, respectively. These values can be used to estimate the C—H bond destruction rate, approximating equation (5) as

$$R_{d,\mathrm{CR}} \simeq \sigma_{d,p}(1\ \mathrm{MeV})\Phi_p(1\ \mathrm{MeV}) \qquad (8)$$

with $\sigma_{d,p}(1\ \mathrm{MeV}) \equiv \sigma_{d,p,1\,\mathrm{MeV}}$ C—H bond destruction cross section for 1 MeV protons.

Substituting equation (6) in equation (8) we can express $R_{d,\mathrm{CR}}$ as a function of ζ_{CR}:

$$R_{d,\mathrm{CR}} \simeq \frac{\sigma_{d,p}(1\ \mathrm{MeV})}{\sigma_{i,p}(1\ \mathrm{MeV})}\zeta_{\mathrm{CR}}\ . \qquad (9)$$

This result indicates that the cosmic-ray C—H bond destruction rate is proportional to the cosmic-ray ionization rate. The factor of proportionality is the ratio between the cross sections at 1 MeV, $\sigma_{d,p}(1\ \mathrm{MeV})/\sigma_{i,p}(1\ \mathrm{MeV})$. In the monoenergetic proton approximation, this factor depends on the energy of protons used to represent the effects of cosmic-ray irradiation[5] and on the environment through the ionization cross section of hydrogen (atomic for diffuse regions and molecular for dense clouds).[6] To analyze the influence of the proton energy on the estimation of $R_{d,\mathrm{CR}}$, we consider the ratio of the cross sections, $r(E)$, as a function of E,

$$r(E) = \frac{\sigma_{d,p}(E)}{\sigma_{i,p}(E)} = \frac{\sigma_{d,p}(1\ \mathrm{MeV})f(E)}{\sigma_{i,p}(1\ \mathrm{MeV})g(E)}\ , \qquad (10)$$

where $f(E)$ and $g(E)$ are, respectively, the C—H bond destruction and ionization cross sections normalized at 1 MeV. The function $f(E)$ is equal to the normalized stopping power of protons in hydrogenated carbon grains. To evaluate $g(E)$ we consider two cases. For dense cloud conditions we adopt the proton impact ionization cross section of H_2 tabulated by Cravens & Dalgarno (1978) from 1 to 100 MeV, while we use the Bethe expression of ionization of atomic hydrogen by protons in the case of diffuse clouds (Spitzer & Tomasko 1968). The normalized value of $r(E)$ at 1 MeV increases slowly with proton energy from 1 up to 1.5 and 1.8 at 100 MeV for H_2 and H, respectively. This result indicates that C—H bond destruction slightly increases with respect to ionization with proton energy. In this respect, the choice of 1 MeV protons to describe, as a first approximation, the effects of cosmic-ray irradiation of hydrogenated carbon grains should be considered a conservative approximation.

To evaluate $\sigma_{d,p,1\,\mathrm{MeV}}$ from our experiments we have to consider the difference between 30 keV He^+ ions and 1 MeV protons in depositing energy in hydrogenated carbon grains. The stopping cross section of 1 MeV protons, $S_{p,1\,\mathrm{MeV}}$, is 260 MeV cm^2 g^{-1}, a factor of 3.2 lower than that of 30 keV He^+ ions (see above). This implies that a fluence of 1 MeV protons a factor of 3.2 higher than that of 30 keV He^+ ions is needed to deposit the equivalent dose. Consequently, the destruction cross sections of C—H bonds by 1 MeV protons are a factor of 3.2 lower than those estimated from the decrease of the 3.4 μm band intensity as a function of 30 keV He^+ ion fluence of Figures 3 and 4. Here we consider the destruction cross section estimated for

[5] For a given environment (i.e., fixed composition of interstellar gas and cosmic-ray spectrum) the proportionality between the cosmic-ray C—H bond destruction rate and the cosmic-ray ionization rate is true in general: $R_{d,\mathrm{CR}} = \alpha\zeta_{\mathrm{CR}}$. The proportionality between these two integral quantities is a consequence of the fact that the same cosmic-ray spectrum produces ionization of gas and C—H bond destruction in hydrogenated carbon materials. The exact evaluation of α is not possible because it would require the knowledge of the ionization and destruction cross sections and the cosmic-ray fluxes.

[6] This dependence reflects the variations of α caused by changes of the gas composition and the cosmic-ray spectrum with environment.

ACARL_H, which, once divided by the factor 3.2, transforms into $(9.4 \pm 0.3) \times 10^{-16}$ cm^2 per 1 MeV proton.

As mentioned above, we can use a different ion to discuss the effects of cosmic-ray irradiation of carbon materials. Here we limit this consideration to helium ions as an example. In this case equation (8) becomes

$$R_{d,\mathrm{CR}} \simeq \frac{\sigma_{d,\mathrm{He}}(2\ \mathrm{MeV})}{\sigma_{i,\mathrm{He}}(2\ \mathrm{MeV})}\zeta_{\mathrm{CR}} \ . \tag{11}$$

We limit to considering atomic hydrogen (diffuse clouds) since in this case we can use the Bethe expression to evaluate the helium impact ionization cross section of atomic hydrogen $\sigma_{i,\mathrm{He}}(2\ \mathrm{MeV})$. Moreover, we adopt 2 MeV because the Bethe expression is valid for ions with an energy in excess of about 0.3 MeV nucleon^{-1} (e.g., Spitzer & Tomasko 1968). Using the C—H bond destruction cross section for 2 MeV helium ions, we find that the factor of proportionality between $R_{d,\mathrm{CR}}$ and ζ_{CR} in equation (11) is a factor of 1.2 lower than the corresponding term in equation (9), which refers to 1 MeV protons.[7] The description of C—H bond destruction in terms of 1 MeV protons or 2 MeV helium ions gives the same result, within a factor of 1.2. Actually, the main source of uncertainty on $R_{d,\mathrm{CR}}$ is that due to ζ_{CR}. The evolution of the interstellar aliphatic component for different values of ζ_{CR} is discussed below. Finally, we want to stress that, although the above reported discussion refers to the cosmic-ray irradiation of carbon grains, it is valid for all the cases in which cosmic-ray processing of ices and refractory grains depends linearly on the stopping power. For example, it is not applicable to ion sputtering.

The evolution of the 3.4 μm band carrier in space under UV and H atom processing has recently been discussed on the basis of laboratory results (Me02). The estimation of the destruction cross section of C—H bonds by cosmic rays allows us to take into account the effects of cosmic-ray processing. In this more general case, the equation governing the evolution is

$$\frac{dn_{\mathrm{CH}}}{dt} = \sigma_f \Phi_{\mathrm{H}}(n_{\mathrm{CH,max}} - n_{\mathrm{CH}}) - \sigma_{d,\mathrm{UV}}\Phi_{\mathrm{UV}} n_{\mathrm{CH}} - \sigma_{d,p,1\ \mathrm{MeV}}\Phi_{p,1\ \mathrm{MeV}} n_{\mathrm{CH}} \ , \tag{12}$$

where n_{CH} is the number of C—H bonds per unit mass of material, $n_{\mathrm{CH,max}}$ is its maximum, Φ_{UV} and $\Phi_{p,1\ \mathrm{MeV}}$ are the UV and 1 MeV proton flux, respectively, $\sigma_{d,\mathrm{UV}}$ and $\sigma_{d,p,1\ \mathrm{MeV}}$ the corresponding C—H bond destruction cross sections, Φ_{H} the H atom flux, σ_f the formation cross section, and t the time.

The general solution of equation (12) is

$$n_{\mathrm{CH}}(t) = \frac{n_{\mathrm{CH,max}}}{1 + (\sigma_{d,\mathrm{UV}}\Phi_{\mathrm{UV}} + \sigma_{d,p,1\ \mathrm{MeV}}\Phi_{p,1\ \mathrm{MeV}})/\sigma_f\Phi_{\mathrm{H}}} \times \left\{1 - \exp\left[-(\sigma_f\Phi_{\mathrm{H}} + \sigma_{d,\mathrm{UV}}\Phi_{\mathrm{UV}} + \sigma_{d,p,1\ \mathrm{MeV}}\Phi_{p,1\ \mathrm{MeV}})t\right]\right\} + n_{\mathrm{CH},i}\exp\left[-(\sigma_f\Phi_{\mathrm{H}} + \sigma_{d,\mathrm{UV}}\Phi_{\mathrm{UV}} + \sigma_{d,p,1\ \mathrm{MeV}}\Phi_{p,1\ \mathrm{MeV}})t\right] \ , \tag{13}$$

where $n_{\mathrm{CH},i}$ is the initial number of C—H bonds. This solution indicates that under simultaneous processing by UV photons, H atoms, and cosmic rays of a carbonaceous material, the equilibrium value of the number of C—H bonds per unit mass of material ($t \rightarrow \infty$),

$$n_{\mathrm{CH},a} = \frac{n_{\mathrm{CH,max}}}{1 + \Gamma} \ , \tag{14}$$

is independent of the initial hydrogenation degree. It is determined by $n_{\mathrm{CH,max}}$ and by the ratio $\Gamma = (\sigma_{d,\mathrm{UV}}\Phi_{\mathrm{UV}} + \sigma_{d,p,1\ \mathrm{MeV}}\Phi_{p,1\ \mathrm{MeV}})/\sigma_f\Phi_{\mathrm{H}}$ between the total destruction rate by photons and ions and the formation rate of C—H bonds by H atoms. The value of $n_{\mathrm{CH,max}}$ depends on the carbon material structure; a reasonable estimation for the maximum hydrogenation of interstellar carbon grains is $(\mathrm{H/C})_{\mathrm{max}} = 1$. Moreover, $n_{\mathrm{CH}}(t)/n_{\mathrm{CH,max}}$ and $(\mathrm{H/C})/(\mathrm{H/C})_{\mathrm{max}}$ differ by less than 3% for $(\mathrm{H/C})_{\mathrm{max}} \leq 1$ (Me02).

The time evolution of grain hydrogenation depends on the environment, since the destruction and formation rates vary in the different regions of the ISM. For the following discussion we adopt $\sigma_{d,\mathrm{UV}} = 1 \times 10^{-19}$ cm^2 photon^{-1} (Me01), $\sigma_f = 1.9 \times 10^{-18}$ cm^2 per H atom (Me02), and the destruction cross section by 1 MeV protons estimated above. Under diffuse medium conditions, we use the UV flux $\Phi_{\mathrm{UV}} = 8 \times 10^7$ photons cm^{-2} s^{-1} (Mathis, Metzger, & Panagia 1983), the hydrogen flux $\Phi_{\mathrm{H}} = 8 \times 10^6$ H atoms cm^{-2} s^{-1} (Sorrell 1990), and the flux $\Phi_{1\ \mathrm{MeV}} = 1.8$ protons cm^{-2} s^{-1} estimated in the present work. Using these values, the destruction rates of C—H bonds by UV photons and 1 MeV protons are 8×10^{-12} s^{-1} and 1.7×10^{-15} s^{-1}, respectively. We note that although $\sigma_{d,p,1\ \mathrm{MeV}} \sim 10^4\sigma_{d,\mathrm{UV}}$, the high UV photon flux in the diffuse medium determines a destruction rate more than 3 orders of magnitude higher than that of cosmic rays. We conclude that the effects of cosmic-ray irradiation on the evolution of the carrier of the aliphatic feature are negligible under diffuse medium conditions. The evolution is governed by the interaction of the carrier of the 3.4 μm band with UV photons and H atoms. In these conditions the solution of equation (12) has been discussed by Me02. Their main conclusion is that the formation of the aliphatic C—H bonds responsible for the absorption at 3.4 μm takes place in the diffuse ISM. The equilibrium value for the degree of hydrogenation is reached in a time interval 3 orders of magnitude shorter than the cloud lifetime, independent of the birth site of carbon dust and of its initial hydrogenation.

In dense regions, the changes of the local environment and those of the grain properties determine the conditions for a gradual dehydrogenation of the carbon particles due to the breakdown of the equilibrium in the competition between formation and destruction of C—H bonds reached in the diffuse medium. In fact, as discussed by Mu01 and Me01, the presence on grains of an ice layer, consisting mainly of water (Gibb et al. 2000), and the reduced amount of atomic hydrogen prevent the formation of C—H bonds by H atoms, while their destruction by UV can proceed. This conclusion relied on the results of UV irradiation of both simple hydrocarbon molecules and hydrogenated carbon particles under simulated dense cloud conditions. Furthermore, in the inner part of dense molecular clouds, most hydrogen is in form of H_2; thus, hydrogenation by H atoms can be neglected because of the reduced amount of atomic hydrogen. The results obtained in the present work provide further support to the validity of that conclusion, indicating a clear destruction of C—H bonds by ion irradiation in hydrogenated carbon particles with an ice cap.

[7] As in the case of protons, the ratio $\sigma_{d,\mathrm{He}}(E)/\sigma_{i,\mathrm{He}}(E)$ slowly increases with E.

In this case the term that represents the C—H bond formation in equation (12) vanishes and $n_{\rm CH}(t)/n_{\rm CH,max}$ decays exponentially with time from its diffuse medium equilibrium value $n_{{\rm CH},a}/n_{\rm CH,max} = 0.66$ (Me02). As discussed in § 3.1, there is a lower limit to the destruction of C—H bonds by ion irradiation. The three irradiation experiments of hydrogenated carbon grains with a water ice cap indicate, at high ion fluences, an average residual intensity of the 3.4 μm band of 13%, or equivalently a reduction of 87%, with respect to the initial intensity. Assuming this value as representative of the residual hydrogenation of interstellar hydrogenated carbon grains, we obtain an asymptotic value of 0.09 for $n_{\rm CH}/n_{\rm CH,max}$. The decay rate is determined by the sum of the destruction rates of C—H bonds by photons and cosmic rays. The former, $R_{d,{\rm UV}}$, decreases exponentially with the visual extinction to the cloud edge, A_V, because of the attenuation of the Galactic field. Water ice accretion starts in quiescent dense regions for a cloud visual extinction $A_{V,C} \simeq 3$ mag (Whittet et al. 2001).[8] In these conditions the value of $R_{d,{\rm UV}}$ is 9×10^{-13} s^{-1}, assuming $A_{\rm UV} = 1.6A_V$.

As stressed by Prasad & Tarafdar (1983), an internal UV flux, $\Phi'_{\rm UV} = 8 \times 10^{19}\zeta_{\rm CR}$ photons cm^{-2} s^{-1}, due to cosmic-ray–induced fluorescence of molecular hydrogen is present in dense regions. These authors obtained $\Phi'_{\rm UV} = 1360$ photons cm^{-2} s^{-1}, assuming $\zeta_{\rm CR} = 1.7 \times 10^{-17}$ s^{-1}. Consistent with the assumption done to estimate $\Phi_{p,1\,{\rm MeV}}$, this requires the use of the same cosmic-ray ionization rate, $\zeta_{\rm CR} = 6 \times 10^{-17}$ s^{-1}, to evaluate $\Phi'_{\rm UV}$. The resulting value, $\Phi'_{\rm UV} = 4.8 \times 10^3$ photons cm^{-2} s^{-1}, is a factor of 3.5 higher than that of Prasad & Tarafdar (1983). It is worth noting that within the limits of validity of the approximations of the monoenergetic cosmic-ray protons and of the description of Prasad & Tarafdar, the total destruction rate of C—H bonds, $R_{d,T}$, due to cosmic rays, $R_{d,{\rm CR}}$, and cosmic-ray–induced UV photons, $R_{d,{\rm UV,int}}$, is proportional to $\zeta_{\rm CR}$:

$$R_{d,T} = R_{d,{\rm UV,int}} + R_{d,{\rm CR}} = \sigma_{d,{\rm UV}} 8 \times 10^{19}\zeta_{\rm CR} + \frac{\sigma_{d,p}(1\ {\rm MeV})}{\sigma_{i,p}(1\ {\rm MeV})}\zeta_{\rm CR} \quad (15)$$

with $\sigma_{i,p}\,(1\ {\rm MeV})$ ionization cross section of molecular hydrogen for 1 MeV protons. Their relative contribution to the destruction of C—H bonds is constant:

$$\frac{R_{d,{\rm UV,int}}}{R_{d,{\rm CR}}} = \frac{8 \times 10^{19}\sigma_{d,{\rm UV}}\sigma_{i,p}(1\ {\rm MeV})}{\sigma_{d,p}(1\ {\rm MeV})}\ . \quad (16)$$

Substituting the numerical values of the cross sections in the previous two relations, we get $R_{d,{\rm UV,int}}/R_{d,{\rm CR}} = 0.5$ and $R_{d,T} = 24.3\zeta_{\rm CR}$, which becomes $R_{d,T} = 1.5 \times 10^{-15}$ s^{-1} for $\zeta_{\rm CR} = 6 \times 10^{-17}$ s^{-1}. This destruction rate equals that by Galactic photons at a depth corresponding to $A_V \simeq 5$ mag.

The evolution with time of grain hydrogenation under UV and ion irradiation is shown in Figure 7 for homogeneous clouds with no internal luminosity source. As A_V increases, the time necessary to obtain a given reduction of the degree of hydrogenation increases because of the attenuation of the external radiation field, and the curves tend to the solid line (see Fig. 7) that represents the evolution due to cosmic-ray irradiation plus the contribution of the internal radiation field. Of course, this means that the destruction of C—H bonds by Galactic UV photons is ineffective inside the cloud and cosmic-ray processing dominates. It is worth noting that, as one can see in Figure 7, the residual degree of hydrogenation after ion processing for the cloud lifetime (3×10^7 yr) is lower than the most stringent upper limit for the reduction of the hydrogenation of the carrier with respect to the diffuse medium conditions (Mu01).

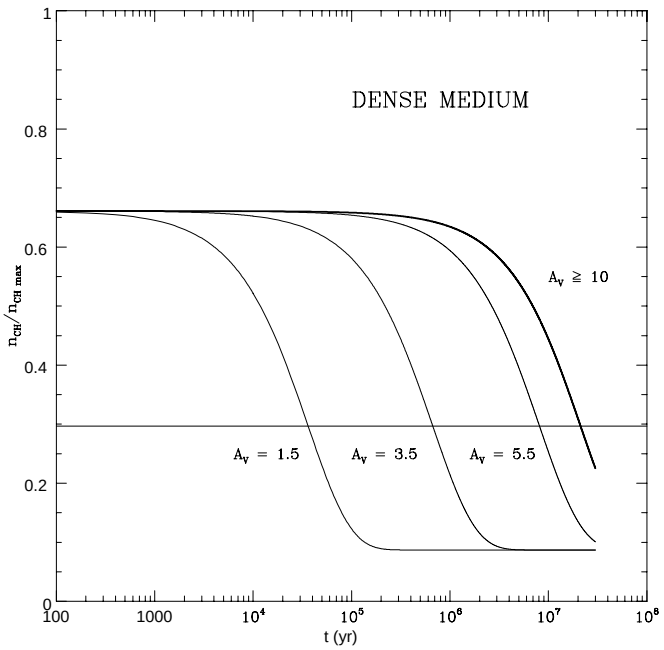

FIG. 7.—Time evolution under dense ISM conditions for hydrogenated carbon grains with an initial degree of hydrogenation as determined by processing in the diffuse ISM. The time $t = 0$ corresponds to the conditions for which hydrogenation of carbon grains is inhibited; see text. The different curves represent the evolution for grains at different depths (A_V) inside the cloud. The thick line refers to the evolution if Galactic UV processing were absent. The horizontal line represents the hydrogenation degree corresponding to the most stringent upper limit for the destruction of the 3.4 μm band in dense regions as determined by Mu01.

The previous results refer to $\zeta_{\rm CR} = 6 \times 10^{-17}$ s^{-1}. Higher values of $\zeta_{\rm CR}$ would accelerate the C—H bond destruction in dense regions. On the other hand, lower cosmic-ray ionization rates would give rise to a lower destruction of the aliphatic component of interstellar carbon grains. The value of $\zeta_{\rm CR}$ corresponding to the most stringent upper limit for C—H bonds in dense clouds is about 4×10^{-17} s^{-1}, which is still compatible, within uncertainties, with the lowest values of $\zeta_{\rm CR}$ inferred from molecular abundances. We would like to note that the previous description of the evolution of C—H bonds refers to homogeneous clouds with no internal luminosity source. However, radially dependent density distribution of clouds, material circulation, and enhancement of intracloud penetration of the Galactic field and cosmic rays in clumpy and filamentary structures can favor grain processing (Cecchi-Pestellini & Aiello 1992; Whittet et al. 1998; Mu01).

The results presented here provide further support to the new interpretation of the difference of the 3.4 μm band in the spectrum of diffuse and dense clouds in terms of an evolutionary transformation of the aliphatic component caused by grain processing. This component is easily formed by H

[8] At a given location in the cloud the extinction to the cloud edge, A_V, is at most equal to one-half the observed total line-of-sight extinction, $A_{V,C}$ (Whittet et al. 1998).

atoms in the diffuse medium and destroyed by UV photons and cosmic rays in dense regions. While destruction occurs in both the dense and diffuse regions, rehydrogenation of carbon materials is inhibited to a significant degree in dense molecular clouds.

This work has been supported by ASI and by MIUR research contracts. We thank S. Inarta, F. Spinella, N. Staiano, and E. Zona for their technical assistance during laboratory measurements. Y. J. P. gratefully acknowledges support by NASA's Exobiology Program 344-38-12-09.

REFERENCES

Adamson, A. J., Whittet, D. C. B., Chrysostomou, A., Hough, J. H., Aitken, D. K., Wright, G. S., & Roche, P. F. 1999, ApJ, 512, 224
Adamson, A. J., Whittet, D. C. B., & Duley, W. W. 1990, MNRAS, 243, 400
Adel, M. E., Amir, O., Kalish, R., & Feldman, L. C. 1989, J. Appl. Phys., 66, 3248
Allamandola, L. J., Sandford, S. A., Tielens, A. G. G. M., & Herbst, T. M. 1992, ApJ, 399, 134
———. 1993, Science, 260, 64
Allamandola, L. J., Sandford, S. A., & Valero, G. J. 1988, Icarus, 76, 225
Bagnulo, S., Doyle, J. K., & Griffin, I. P. 1995, A&A, 301, 501
Baratta, G. A., Arena, M. M., Strazzulla, G., Colangeli, L., Mennella, V., & Bussoletti, E. 1996, Nucl. Instrum. Methods Phys. Res. B, 116, 195
Baratta, G. A., Leto, G., Spinella, F., Strazzulla, G., & Foti, G. 1991, A&A, 252, 421
Brooke, T. Y., Sellgren, K., & Geballe, T. R. 1999, ApJ, 517, 883
Brooke, T. Y., Sellgren, K., & Smith, R. G. 1996, ApJ, 459, 209
Cecchi-Pestellini, C., & Aiello, S. 1992, MNRAS, 258, 125
Chiar, J. E., Adamson, A. J., Pendleton, Y. J., Whittet, D. C. B., Caldwell, D. A., & Gibb, E. L. 2002, ApJ, 570, 198
Chiar, J. E., Adamson, A. J., & Whittet, D. C. B. 1996, ApJ, 472, 665
Chiar, J. E., Pendleton, Y. J., Geballe, T. R., & Tielens, A. G. G. M. 1998, ApJ, 507, 281
Chiar, J. E., Tielens, A. G. G. M., Whittet, D. C. B., Schutte, W. A., Boogert, A. C. A., Lutz, D., van Dishoeck, E. F., & Bernstein, M. P. 2000, ApJ, 537, 749
Colangeli, L., Mennella, V., Palumbo, P., Rotundi, A., & Bussoletti, E. 1995, A&AS, 113, 561
Compagnini, G., & Calcagno, L. 1994, Mat. Sci. Eng., 5(6), 193
Compagnini, G., Calcagno, L., & Foti, G. 1992, Phys. Rev. Lett., 69, 454
Cravens, T. E., & Dalgarno, A. 1978, ApJ, 219, 750
de Jong, T., & Kamijo, F. 1973, A&A, 25, 363
Dillon, R. O., Woollam, J. A., & Katkanant, V. 1984, Phys. Rev. B, 29, 3482
Federman, S. R., Weber, J., & Lambert, D. L. 1996, ApJ, 463, 181
Fujimoto, F., Tanaka, M., Iwata, Y., Ootuka, A., Komaki, K., Haba, M., & Kobayashi, K. 1988, Nucl. Instrum. Methods Phys. Res. B, 33, 792
Gibb, E. L., et al. 2000, ApJ, 536, 347
Gonzalez-Hernandez, J., Asomaza, R., Reyes-Mena, A., Rickards, J., Chao, S. S., & Pawlik, D. 1988, J. Vac. Sci. Technol. A, 6, 1798
Greenberg, J. M. 1978, in Cosmic Dust, ed. J. A. M. McDonnell (New York: Wiley), 187
Greenberg, J. M., Li, A., Mendoza-Gomez, C. X., Schutte, W. A., Gerakines, P. A., & De Groot, M. 1995, ApJ, 455, L177
Imanishi, M. 2000, MNRAS, 319, 331
Imanishi, M., & Dudley, C. C. 2000, ApJ, 545, 701
Jenniskens, P., Baratta, G. A., Kouchi, A., de Groot, M. S., Greenberg, J. M., & Strazzulla, G. 1993, A&A, 273, 583
Johnson, R. E. 1990, Energetic Charged Particle Interactions with Atmospheres and Surfaces (Berlin: Springer)
———. 1998, in Solar System Ices, ed. B. Schimitt, C. De Bergh, & M. Festou (Dordrecht: Kluwer), 303
Jones, A. P., Tielens, A. G. G. M., Hollenbach, D. J., & Mckee, C. F. 1994, ApJ, 433, 797
Kalish, R., & Adel, M. E. 1989, Mat. Sci. Forum, 52, 427
Keane, J. V., Tielens, A. G. G. M., Boogert, A. C. A., Schutte, W. A., & Whittet, D. C. B. 2001, A&A, 376, 254
Kulkarni, S. R., & Heiles, C. 1987, in Interstellar Processes, ed. D. J. Hollenbach & H. A. Thronson, Jr. (Dordrecht: Reidel), 87
Lequeux, J., & Jourdain de Muizon, M. 1990, A&A, 240, L19
Mathis, J. S., Mezger, P. G., & Panagia, N. 1983, A&A, 128, 212
McKee, C. F. 1989, in Interstellar Dust, ed. L. J. Allamandola & A. G. G. M. Tielens (Dordrecht: Kluwer), 431
Mennella, V., Baratta, G. A., Colangeli, L., Palumbo, P., Rotundi, A., Bussoletti, E., & Strazzulla, G. 1997, ApJ, 481, 545
Mennella, V., Brucato, J. R., Colangeli, L., & Palumbo, P. 1999, ApJ, 524, L71 (Me99)
———. 2002, ApJ, 569, 531 (Me02)
Mennella, V., Colangeli, L., Bussoletti, E., Monaco, G., Palumbo, P., & Rotundi, A. 1995, ApJS, 100, 149
Mennella, V., Muñoz Caro, G., Ruiterkam, R., Schutte, W. A., Greenberg, J. M., Brucato, J. R., & Colangeli, L. 2001, A&A, 367, 355 (Me01)
Moore, M. H. 1999, in Solid Interstellar Matter: The ISO Revolution, ed. L. d'Hendecourt, C. Joblin, & A. Jones (Berlin: Springer), 199
Moore, M. H., & Donn, B. 1982, ApJ, 257, L47
Moore, M. H., Hudson, R. L., & Gerakines, P. A. 2001, Spectrochim. Acta A, 57, 843
Muñoz Caro, G., Ruiterkam, R., Schutte, W. A., Greenberg, J. M., & Mennella, V. 2001, A&A, 367, 347 (Mu01)
Pendleton, Y. J. 1995, Planet. Space Sci., 43, 1359
———. 1996a, in The Cosmic Dust Connection, ed. J. M. Greenberg (Dordrecht: Kluwer), 71
———. 1996b, in New Extragalactic Perspectives in the New South Africa, ed. D. Block & J. M. Greenberg (Dordrecht: Kluwer), 135
Pendleton, Y. J., & Allamandola, L. J. 2002, ApJS, 138, 75
Pendleton, Y. J., Sandford, S. A., Allamandola, L. J., Tielens, A. G. G. M., & Sellgren, K. 1994, ApJ, 437, 683
Prasad, S. S., & Tarafdar, S. P. 1983, ApJ, 267, 603
Reynaud, C., Guillois, O., Herlein-Boime, N., Rouzaud, J.-N., Galvez, A., Clinard, C., Balanzat, E., & Ramillon, J.-M. 2001, Spectrochim. Acta A, 57, 797
Robertson, J. 1991, Prog. Solid State Chem., 21, 199
Rotundi, A., Rietmeijer, F. J. M., Colangeli, L., Mennella, V., Palumbo, P., & Bussoletti, E. 1998, A&A, 329, 1087
Sandford, S. A., Allamandola, L. J., Tielens, A. G. G. M., Sellgren, K., Tapia, M., & Pendleton, Y. 1991, ApJ, 371, 607
Simpson, J. A. 1983, Annu. Rev. Nucl. Part. Sci., 33, 323
Sorrell, W. H. 1990, MNRAS, 243, 570
Spitzer, L., Jr., & Tomasko, M. G. 1968, ApJ, 152, 971
Strazzulla, G. 1998, in Solar System Ices, ed. B. Schimitt, C. De Bergh, & M. Festou (Dordrecht: Kluwer), 281
Strazzulla, G., Baratta, G. A., Leto, G., & Foti, G. 1992, Europhys. Lett., 18, 517
Strazzulla, G., Baratta, G. A., & Palumbo, M. E. 2001, Spectrochim. Acta A, 57, 825
Strazzulla, G., & Johnson, R. E. 1991, in Comets in the Post-Halley Era, ed. R. L. Newburn, M. Neugerbauer, & J. Rahe (Dordrecht: Kluwer), 243
Tamor, M. A., Haire, J. A., Wu, C. H., & Hass, K. C. 1989, Appl. Phys. Lett., 54, 123
Tielens, A. G. G. M., Wooden, D. H., Allamandola, L. J., Bregman, J., & Witteborn, F. C. 1996, ApJ, 461, 210
Tuinstra, F., & Koenig, J. L. 1970, J. Chem. Phys., 53, 23
van der Tak, F. F. S., & van Dishoeck, E. F. 2000, A&A, 358, L79
Wickramasinghe, D. T., & Allen, D. A. 1980, Nature, 287, 518
Whittet, D. C. B., Gerakines, P. A., Hough, J. H., & Shenoy, S. S. 2001, ApJ, 547, 872
Whittet, D. C. B., et al. 1997, ApJ, 490, 729
———. 1998, ApJ, 498, L159
Wild, Ch., & Koidl, P. 1987, Appl. Phys. Lett., 51, 1506
Willner, S. P., Russell, R. W., Puetter, R. C., Soifer, B. T., & Harvey, P. M. 1979, ApJ, 229, L65
Wright, G., Geballe, T., Bridger, A., & Pendleton, Y. J. 1996, in New Extragalactic Perspectives in the New South Africa, ed. D. Block & J. M. Greenberg (Dordrecht: Kluwer), 143